*Research Note*

# Assessing the Safety of Reticular Double Layer Domes with/without Primary Consideration of Equivalent Static Earthquake Loading

***Arjang Sadeghi[1*] and Amin Sadr-Noormohammadi[2]***

1. Assistant Professor, Civil Engineering Department, Azarbaijan Shahid Madani University, Tabriz, * Corresponding Author; email: a.sadeghi@azaruniv.edu
2. M.Sc. in Structural Engineering

**Received:** 16/12/2012
**Accepted:** 28/01/2014

## ABSTRACT

*Reticular double layer domes have gained in huge popularity for their lightness, easy construction and repair, highly indeterminacy and efficiency in covering large spaces. Although this kind of space structures is employed widely in practice, there is not enough information about their seismic design procedure. Among the works carried out in quantifying the earthquake effects on the double layer domes, one can refer to the work done by authors in 2010. They presented some equations for estimation of equivalent static loadings on double layer domes. The present paper aims at investigating the efficiency of these equations through comparing the dynamic nonlinear responses of two sets of domes that are designed with and without consideration of these loadings in design stage. The result of the analyses shows that although these equations improve the responses of the considered domes, they do not make them absolutely safe.*

**Keywords:**
Space structures;
Double layer domes;
Dynamic analysis;
Finite element

## 1. Introduction

Space structures such as double layer domes or barrel vaults are widely used in covering large spaces. While the static and dynamic properties of these structures are studied vastly, there are not generally accepted design methods in practice. Since the space structures are generally light and consist of considerably redundant members, for a while they were supposed to be seismic structures. The Kobe earthquake of 1995 in Japan happened in a region with many space structures in use and showed that although the vulnerability of space structures are less; they should not be counted on as safe structures. The relatively low damages were taken important since the sites covered by space structures were utilized as temporary shelters for home-lost people in earthquake hit areas. Since then, considerable amount of efforts are focused on assessing the seismic behavior of space structures and quantifying the seismic action on these structures. Here, a few of research that carried out on seismic behavior of space structures are listed.

Saka et al. [1] reported the damages of some space structures experiencing the Kobe 1995 earthquake. Kawaguchi [2] also reported more damages in the roofs of sport areas covered by space structures during the same event. Sokol et al. [3] investigated the seismic behavior of a single layer lattice dome and concluded that the maximum induced forces and stresses are sensitive to the influence of rotation components of seismic input. Malek et al. [4] studied the seismic behavior of a

triple layer grid against El Centro earthquake of 1943 and concluded that although the numeric difference between the effects of single and triple components of that earthquake on the grid are important, total failure is not expectable for events in such strength. Ishikawa and Kato [5] presented a semi-dynamic method to model the earthquake loading on single layer domes. In another attempt, in China, a code of practice was issued that concluded an equivalent static earthquake loading on double layer grids [6]. Sadeghi [7-9] investigated the seismic behavior of double layer barrel vaults and presented some formula for modeling earthquake loading statically on these structures. These formulae were validated later in another paper and the results of numerous nonlinear dynamic analyses showed that considering those formulae during design stage improved the responses of double layer barrel vaults significantly [10 ]. However, there is still more space to develop these equations to make them more versatile. Ma and Yao [11] investigated the dynamic characteristics of a single-layer reticular shell stressed by tendons; however, this study did not conclude a seismic analysis. Shen et al. [12] studied on the seismic behavior of single layer barrel vaults and presented a modification factor method for modeling the static seismic effect on these structures. This method is similar to the code of practice of China method unless it is for the single layer barrel vaults. Salajegheh et al. [13] investigated the seismic behavior of double layer barrel vaults by performance based method and concluded that the structures designed according to a specific seismic demand would perform satisfactorily during strong ground motions. Moghaddam [14] studied the seismic behavior of some modules of double layer barrel vaults and concluded that these structures behave very safely during strong earthquakes; however, he reported considerable horizontal displacements in these modules. Cai et al. [15] studied the dynamic behavior of a cable dome and concluded that the principle modes of these structures are vertical ones.

In the current paper, the aim is to supply some formulae for equivalent static earthquake loading on the double layer domes to ease the design stage of these structures and to verify the versatility of application of these formulae in the design of double layer domes, the primary report of the first stage of this research is presented already [16].

## 2. Configuration of Selected Double Layer Domes

In this research, some double layer dome models with fixed span of 40 m and rise to span ratios of 0.1, 0.2, 0.3, 0.4 and 0.5 are constructed. All the peripheral low layer joints are fixed as simple supports against transitions in all directions. The distance of two layers is assumed as 1 m, for all models. Figure (1) illustrates the general layout of the selected models.

The members sections are selected from tubular pipe sections and are proportioned according to AISC-ASD1988. Their slenderness ratio is kept constant as 100. Loading is applied according to section 6 of National Housing Requirements of Iran [17]. In this regard, the snow loading is taken as 1500 N/m$^2$ and is applied in symmetric and asymmetric patterns. The dead load is taken as 500 N/m$^2$ and is applied as concentrated loads on the upper layer joints. For design purposes, analyses package of SAP2000 is utilized. However, for nonlinear dynamic analysis where post-buckling behavior is important, the powerful finite element package of ANSYS is employed. For analysis purposes in the ANSYS, the element LINK180 is used for modal

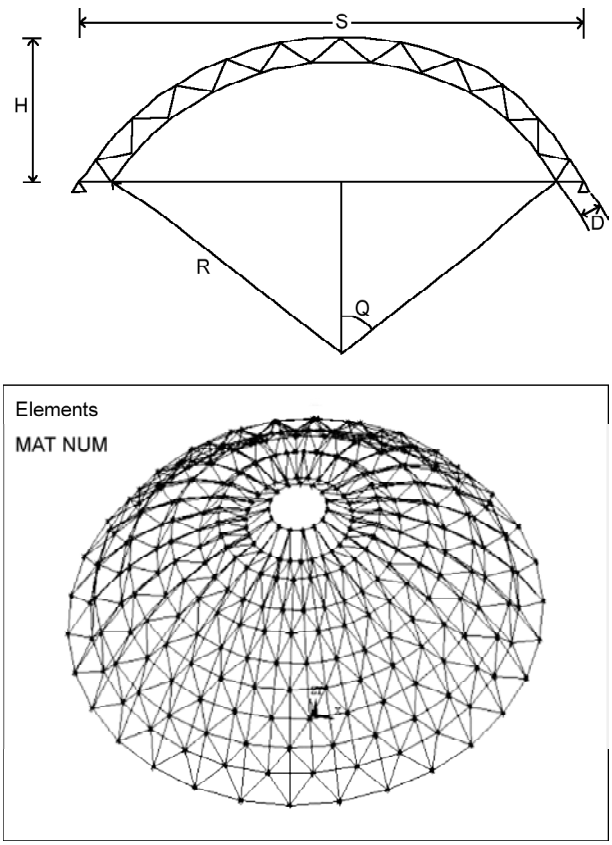


**Figure 1.** General layout of double layer domes models

analysis of the dome elements. COMBIN39 is used for dynamic and nonlinear behavior of the elements [18]. The nonlinearity is considered in both material and geometry of the models.

The physical and mechanical properties of the steel material are introduced as: $E = 2.1E11$ N/m$^2$, $\nu = 0.3$, $\rho = 7850$ kg/m$^3$, $F_y = 2.4E8$ N/m$^2$ and $F_u = 3.6E8$ N/m$^2$.

## 3. Horizontal Equivalent Static Load of Earthquake on Double Layer Domes

### 3.1. Dynamic Analyses of Models

To accomplish this research, four strong ground motions are selected, Table (1). The selected earthquakes have got high response for the short period structures like double layer domes. The horizontal acceleration records of these earthquakes are scaled according to the code of practice of seismic design of buildings of Iran [19]. The site of the structure is assumed to be located in a very high seismic risk and the soil type is assumed as type 2 (with shear wave speed greater than 75 m/s). The damping ratio of the standard response spectra is 5%, so they are corrected for the domes with the damping ratio of 2% by the following formula [20]:

$$S_a(\xi) = S_a(5\%) \times \sqrt{\frac{10}{\xi + 5}} \tag{1}$$

At first, to obtain the dynamic characteristics of the double layer domes, a set of eigen-value analyses were carried out and then the Rayleigh damping coefficients were calculated from the following formulae [21]:

$$[C] = \alpha[M] + \beta[K] \tag{2}$$

$$\alpha = \xi \frac{2 f_i f_j}{f_i + f_j}$$
$$\beta = \xi \frac{2}{f_i + f_j} \tag{3}$$

The $i^{th}$ mode is taken as the first effective horizontal mode and the $j^{th}$ mode is the farthest mode from the $i$ mode with mass participation factor of nearly 10% or more.

**Table 1.** Selected accelerograms general characteristics.

| **Earthquake** | **Tabas, Iran 1978/09/16 (H)** | **Tabas, Iran 1978/0/16 (V)** |
|---|---|---|
| Record/Component | Tabas/TAB-TR | TABAS/TAB-UP |
| HP (Hz) | 0.05 | 0.05 |
| LP (Hz) | Null | Null |
| PGA (g) | 0.852 | 0.688 |
| PGV (cm/s) | 121.4 | 98.03 |
| PGD (cm) | 94.58 | 76.37 |
| **Earthquake** | **Tabas, Iran 1978/09/16 (H)** | **Tabas, Iran 1978/0/16 (V)** |
| Record/Component | IMPVALL/I-ELC180 | IMPVALL/I-ELC-UP |
| HP (Hz) | 0.2 | 0.2 |
| LP (Hz) | 15 | 15 |
| PGA (g) | 0.313 | 0.205 |
| PGV (cm/s) | 29.8 | 10.7 |
| PGD (cm) | 13.32 | 9.16 |
| **Earthquake** | **Kobe, Japan 1995/01/16 (H)** | **Kobe, Japan 1995/01/16 (V)** |
| Record/Component | KOBE/KJM000 | KOBE/KJM-UP |
| HP (Hz) | 0.05 | 0.05 |
| LP (Hz) | Null | Null |
| PGA (g) | 0.821 | 0.343 |
| PGV (cm/s) | 81.3 | 38.3 |
| PGD (cm) | 17.68 | 10.29 |
| **Earthquake** | **Duzce, Turkey 11/12/99 (H)** | **Duzce, Turkey 11/12/99 (V)** |
| Record/Component | DUZCE/375-N | DUZCE/375-V |
| HP (Hz) | 0.15 | 0.06 |
| LP (Hz) | 50 | 50 |
| PGA (g) | 0.97 | 0.193 |
| PGV (cm/s) | 36.5 | 9.5 |
| PGD (cm) | 5.48 | 6.2 |

### 3.2. Earthquake Coefficient Assessment

The first step for establishing an equivalent static loading on the double layer domes is to assess the resultant base shear ($V_b$) on the double layer domes. The customary equivalent static seismic relation, Eq. (5), is adopted for this purpose:

$$V_b = C_H \times W_t \tag{5}$$

where $C_H$ is the horizontal earthquake loading coefficient and $W_t$ is the effective weight of the structure.

From Eq. (5), one can calculate the horizontal coefficient, $C_H$, in the following form:

$$C_H = \frac{V_b}{W_t} \tag{6}$$

On the other hand, the earthquake coefficient is related to the normalized dynamic response of the system in the principle mode, Eq. (7). Of course, this assumption is correct in the linear behavior region. Considering the Eqs. (6) and (7), one can establish the Eq. (8) in which:

$$C_H = \alpha \frac{S_a(T_m)}{g} \quad (7)$$

where α is a coefficient. Thus:

$$\alpha = \frac{g \times C_H}{S_a(T_m)} \quad (8)$$

For calculation of α, the entire selected double layer dome models are analyzed linearly under the 4 chosen and scaled accelerograms. Then the resulted horizontal base shears are extracted and put in Eq. (6) to obtain corresponding $C_H$. Then, by dividing $C_H$ by the response acceleration of each dome, the corresponding α is calculated, Eq. (8). In consequence, a graph illustrating the relation between this coefficient and the rise to span ratios of the domes is constructed, Figure (2). Finally, a relationship is fitted for the average of α as:

$$\alpha = -0.668\left(H/S\right) + 1.535 \quad (9)$$

By Eq. (9), one can easily find α for every double layer domes with specific rise to span ratio and put the value into Eq. (7) to calculate the horizontal earthquake coefficient $(C_H)$ and eventually obtain the horizontal base shear acting on a double layer dome by Eq. (5). The result may be presented in brief as:

$$V_b = \alpha \frac{S_a(T_m)}{g} W_t \quad (10)$$

Comparison of Eq. (10) with conventional earthquake static loading of buildings shows that:

$$\alpha \frac{S_a(T_m)}{g} = \frac{ABI}{R} \quad (11)$$

Since $S_a(T_m) = B$ and is extracted from the design spectrum of the seismic codes and taking $I = 1$, then alpha appears to be equal to:

$$\alpha = \frac{g.A}{R} \quad (12)$$

In effect, taking alpha = 1.4 from Figure (2), $g$= 10 cm/s$^2$ and $A$=0.35 for a high seismic region, Eq. (12) leads to a behavior factor of around 2.5 for a double layer dome. Of course, this figure is inherent in Eq. (10).

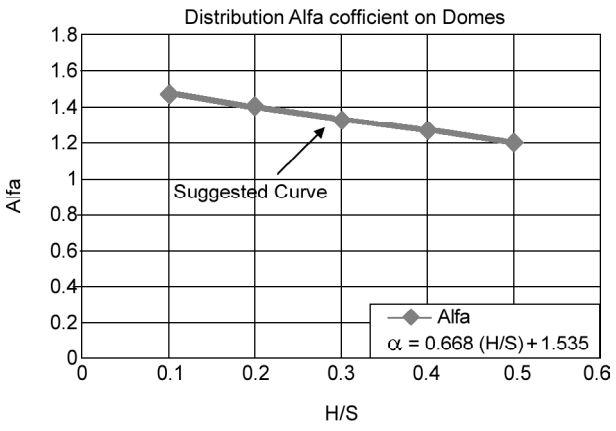


**Figure 2.** Fitted curve for coefficient α.

### *3.3. Distribution of Base Shear in the Height of a Dome*

Having the equivalent static base shear in hand, the second step is to distribute it in the height of a double layer dome. For this purpose, at first, the pattern of vertical distribution of base shear is constructed. To establish this pattern, the mass of each joint on the upper layer of the reticular domes are multiplied by their proportional acceleration responses. Then, the resulted products are summed up for the joints of each level ($j$) of the domes. Eq. (13) represents this action:

$$F_i = \left|\sum m_i \times (\ddot{u})\right| \quad (13)$$

where $F_j$ is the total inertial force of level $j$, $i$ is the number of joint of level $j$ and $m_i$, and refers to mass and response proportional acceleration of joint $i$ of the dome.

Then, four sets of $F_j$ are ready in hand for four selected earthquakes for each double layer dome with specific rise to span ratio. The heights $(h_j)$ of each level are normalized to the total height of each dome, $H$. To have a general pattern, the forces of the joint levels of the domes are normalized to the maximum magnitude of each analysis. Then, the normalized level forces of four earthquakes are averaged for each dome, which is shown by bold lines in Figurs (3) to (5a). The average normalized level forces are collected in a graph, Figure (5b). The graph illustrates that the vertical distribution pattern of earthquake loadings in the height of double layer domes with different rise to span ratios are effectively similar. Finally, for presenting a meaningful unique relationship for vertical earthquake loading pattern for all double layer domes, the curves are averaged again (the dashed line in Figure (5b)). The resulted curve gives the general pattern for the distribution of the earthquake equivalent static base shear in the height of a reticular dome.

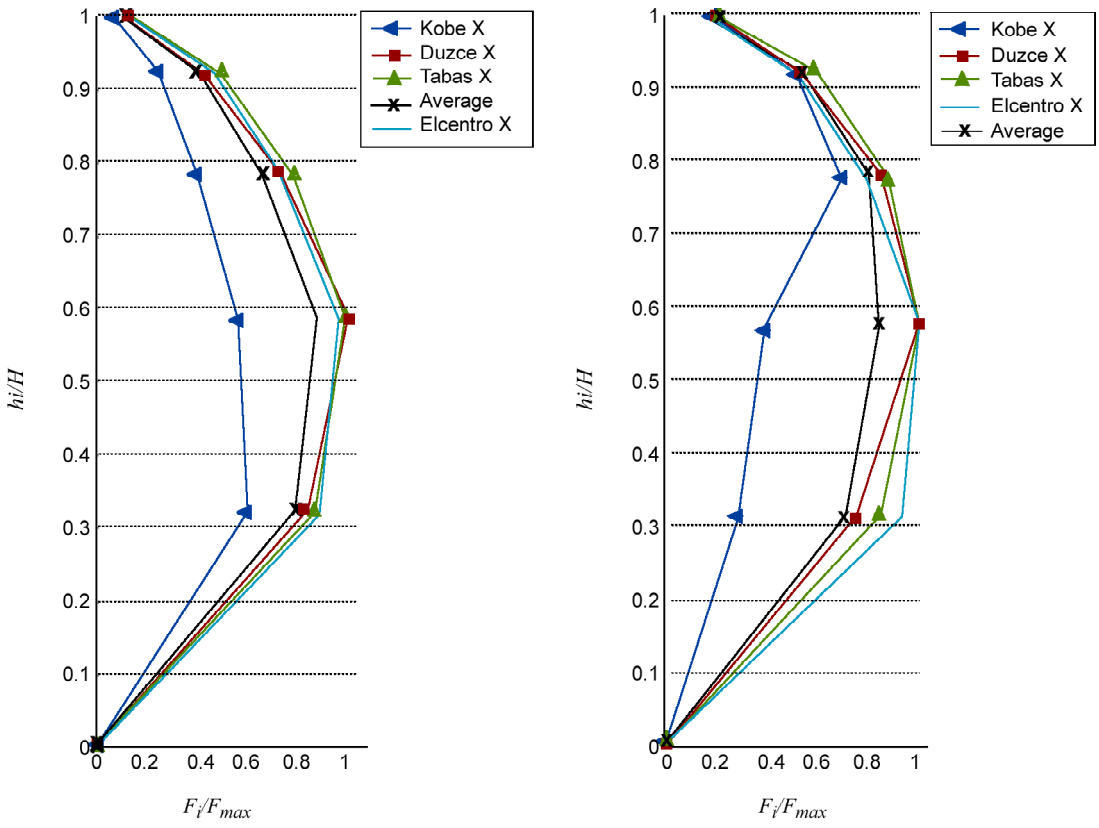


(a) Rise to Span Ratio of 0.3 (b) Rise to Span Ratio of 0.4

**Figure 3.** Earthquake loading distribution pattern in height of domes with rise to span ratios of 0.1 and 0.2.

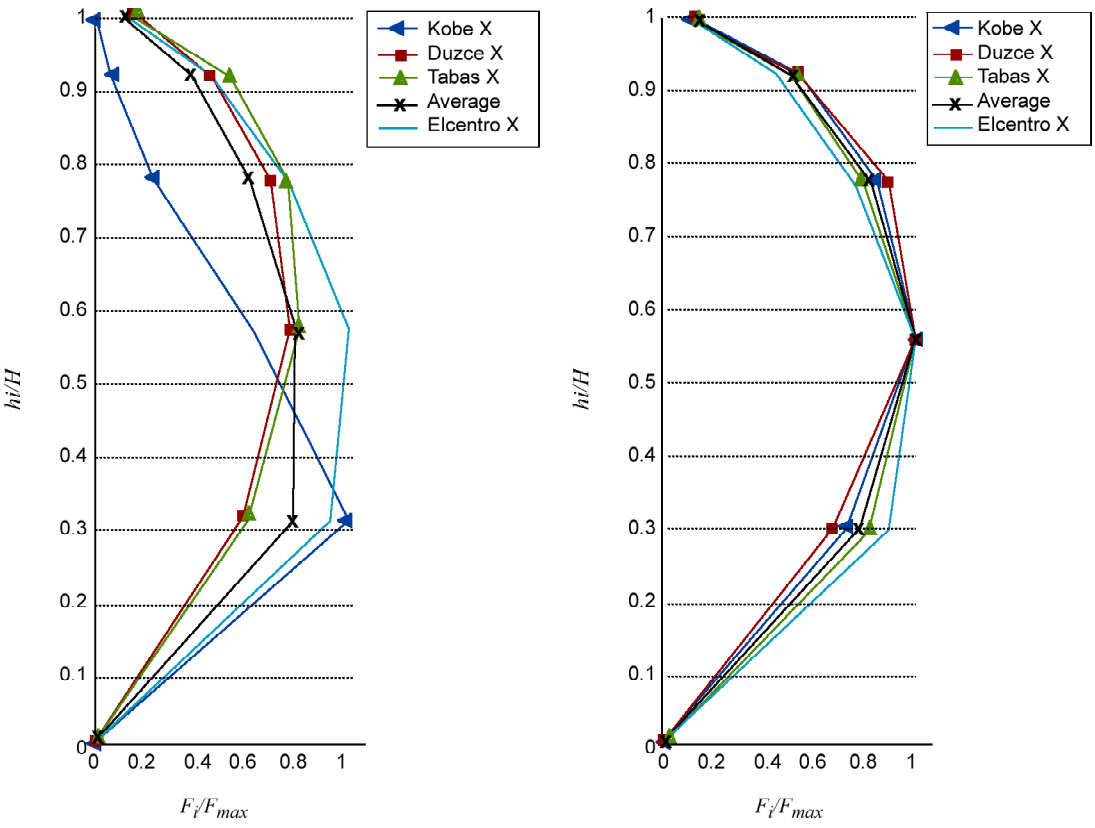


(a) Rise to Span Ratio of 0.3 (b) Rise to Span Ratio of 0.4

**Figure 4.** Earthquake loading distribution pattern in height of domes with rise to span ratios of 0.3 and 0.4.

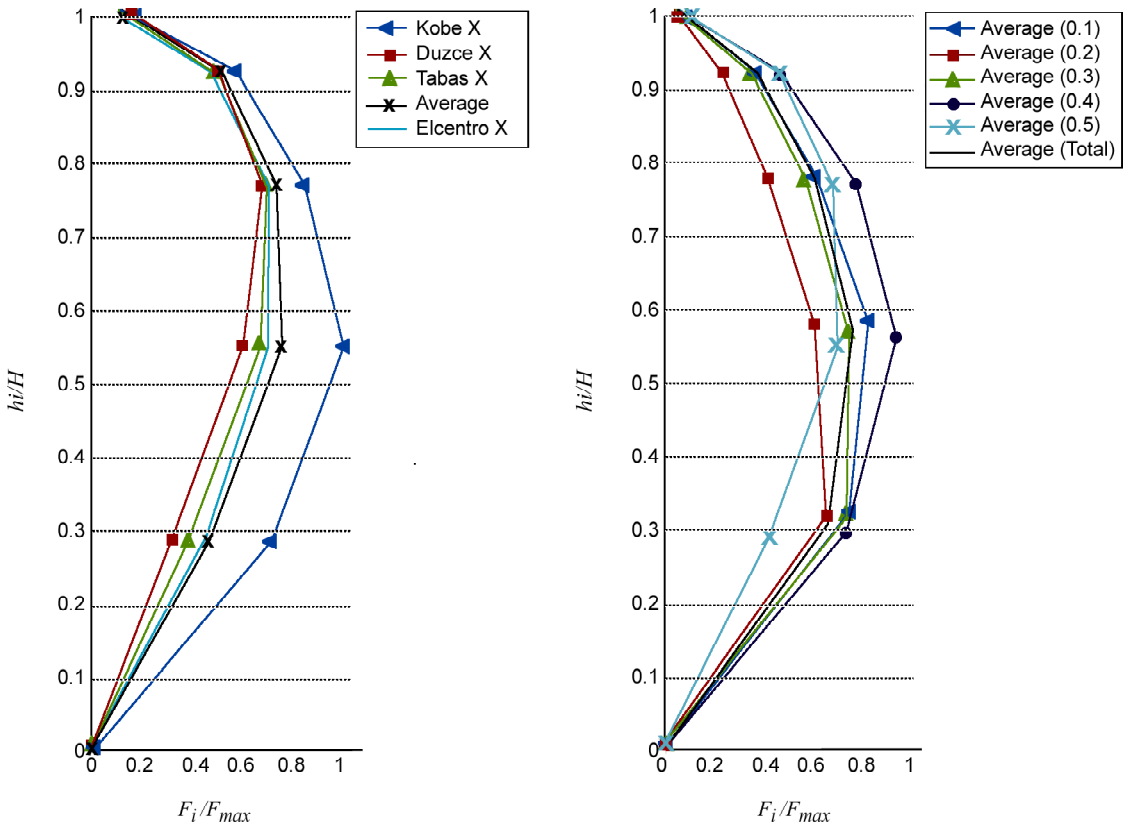


**Figure 5.** Earthquake loading distribution pattern in height of dome with rise to span ratios of 0.5 and averaged normalized pattern for all domes.

To simplify the pattern for design purposes, the resulted general pattern obtained from Figure (5b) is shown again in Figure (6) and is replaced by a simple three-line curve (light color in Figure (6)). In the fitted curve for the loading pattern, the left hand areas of the curves are kept equal. The aim of using a three-line curve is to obtain a unique pattern of loading distribution in the height of all double layer domes. The fitted equations for the vertical distribution of equivalent static loading are as follows:

$$F_j = \frac{\left(\frac{h_i}{H}\right)}{0.3} \times Y \qquad 0 \le \left(\frac{h_j}{H}\right) \le 0.3$$

$$F_j = Y \qquad 0.3 < \left(\frac{h_j}{H}\right) < 0.8 \qquad (14)$$

$$F_j = \frac{1.037 - \left(\frac{h_i}{H}\right)}{0.237} \times Y \qquad 0.8 \le \left(\frac{h_j}{H}\right) \le 1$$

The required parameters can be calculated from the following equations:

$$Y = \frac{V_b}{(a+n+b)}$$

$$a = \sum_{0}^{0.3} \frac{\left(\frac{h_j}{H}\right)}{0.3} \qquad (15)$$

$$b = \sum_{0.8}^{1} \frac{\left(1.037 - \left(\frac{h_j}{H}\right)\right)}{0.237}$$

where $F_j$ is the lateral earthquake load for level $j$, $h_j$ is the height of level $j$, $H$ is the total height of the dome from the ground level, $V_b$ is the earthquake equivalent static base shear at the ground level for a double layer dome, Eq. (5), and $n$ is the number of joints levels of a dome in the range of $0.3 < h_j/H < 0.8$.

It should be noted that the extracted vertical distribution pattern of earthquake loadings are based

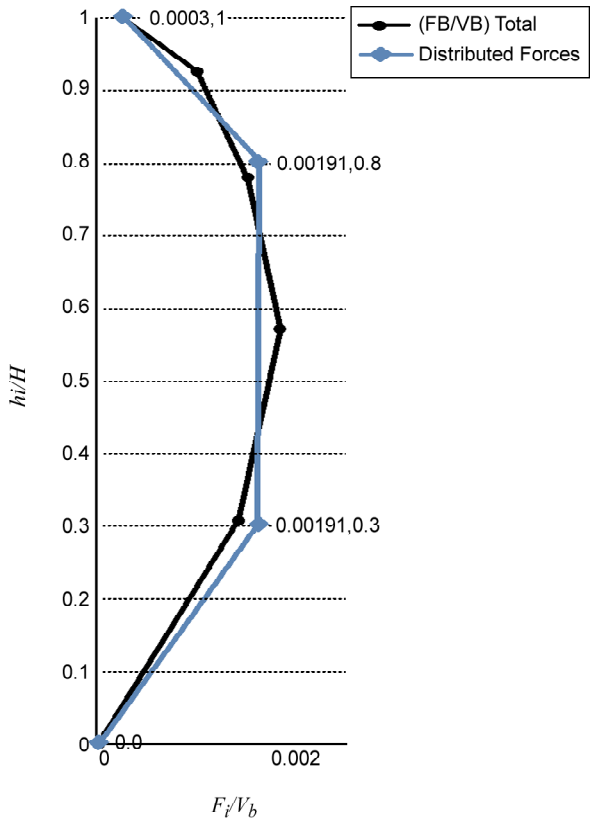


**Figure 6.** Vertical distribution curve of base shear and fitted curve.

on the inertial forces of domes, which are just a part of total dynamic forces. It is clear that, although this method may present a satisfactory pattern of load distribution for inertial forces in the height of the domes, it is inherent with approximations for total dynamic forces. Furthermore, this pattern has no similarity to the effective modes of double layer domes. Despite the ordinary buildings that the shape of first mode - as the dominant mode, is adapted as the vertical load distribution pattern, the double layer domes have no dominant mode and usually there are several modes that are more or less simultaneously effective. Therefore, for double layer domes, it is not logic to use the shape of any mode as the vertical or horizontal load distribution pattern. Consequently, this method is presented for obtaining a reasonable and applied vertical distribution of earthquake equivalent static loading pattern on double layer domes.

### *3.4. Horizontal Distribution of Level Loads*

The level forces, $F_j$, obtained by Eq. (14) are the total lateral loads for each level. For design purposes, this load should be distributed among the joints of that level properly. To get the proper pattern of horizontal distribution of level loads among the joints of that level, the inertial loads of the joints of each level were extracted separately and were normalized to the maximum amount in the relevant level and then were averaged for each dome, level by level. Then, the averages of normalized forces of each level were averaged for all domes to get a general pattern for horizontal distribution of lateral load among the joints of each level of double layer domes. Finally, a two-line curve was fitted for the horizontal pattern of distribution of loads on a level's joints, Figure (7). It should be noted that Figure (7) shows only one half of the distributed level forces and the rest of the nodes are affected symmetrically. Eq. (16) presents the equivalent static earthquake loads for any joint, *i*, of any level, *j*, of a double layer dome.

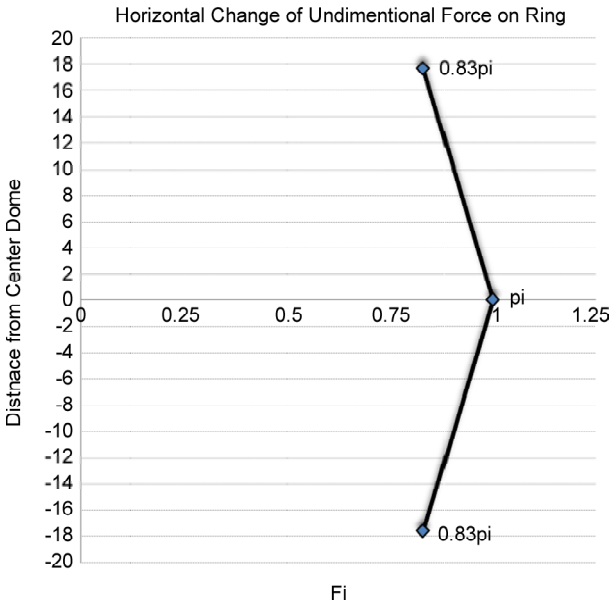


**Figure 7.** Two line distribution Pattern of normalized forces in a level.

$$P_i = \frac{F_j}{N} \times \left(1.11 - 0.17 \times \left| Sin \frac{360}{N} \times i \right|\right), \quad 0 \le i \le N \tag{16}$$

where $i$ is the situation of the specified joint, Figure (8) and varies from 0 to $N$, $N$ is the number of divisions of each level of the dome, $F_j$ is the total lateral load for level $j$ (Equation), and $P_i$ is the imposed lateral load for joint i in level $j$.

## 4. Verifying the Versatility of Presented Equivalent Static Earthquake Loading in Double Layer Domes

### *4.1. Selected Models*

To investigate the versatility of Eqs. (5), (12) and (14) presented by the authors, two sets of double layer domes with the same geometry and configuration were selected. The elements of first set of models were proportioned against necessary combinations of dead and snow loadings (named as DD models), while the elements of the second set of models were proportioned against more load combinations concluding earthquake equivalent static loadings presented in this paper (named as DE models). For consideration of the stability of the two sets of models against earthquakes records, nonlinear analysis were carried out and for this purpose post-buckling behavior of elements of both models was adapted from the pattern, Figure (9) established by Ishikawa and Kato [5].

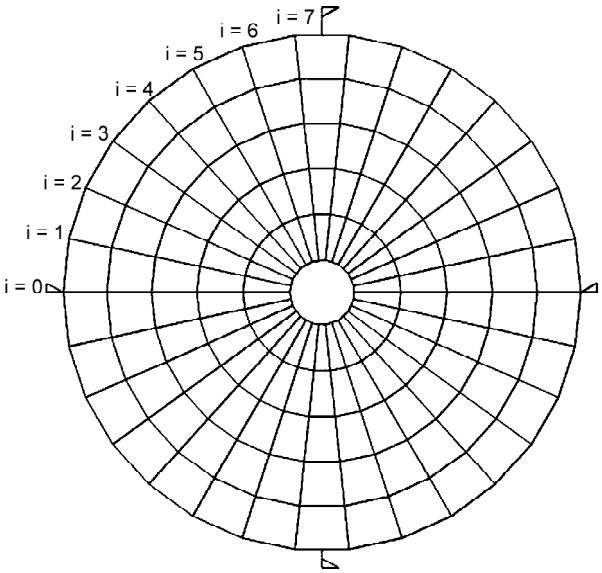


**Figure 8.** Layout of joints numbers of a double layer dome.

Again, the damping ratio in the models was taken as 2% for all models and introduced to the software through the Raleigh coefficients. In this regard, the boundary modes are taken as the first and last mode with high mass participation ratio (more than 10%). The Eigen-value analyses results, Figures (10) and (11), show that the consideration of earthquake loading in the design stage of double layer domes results in diminishing of periods of the domes, which is of course predictable. This reduction is about 10% for the studied models of this research and is concentrated mostly in the primary modes that are

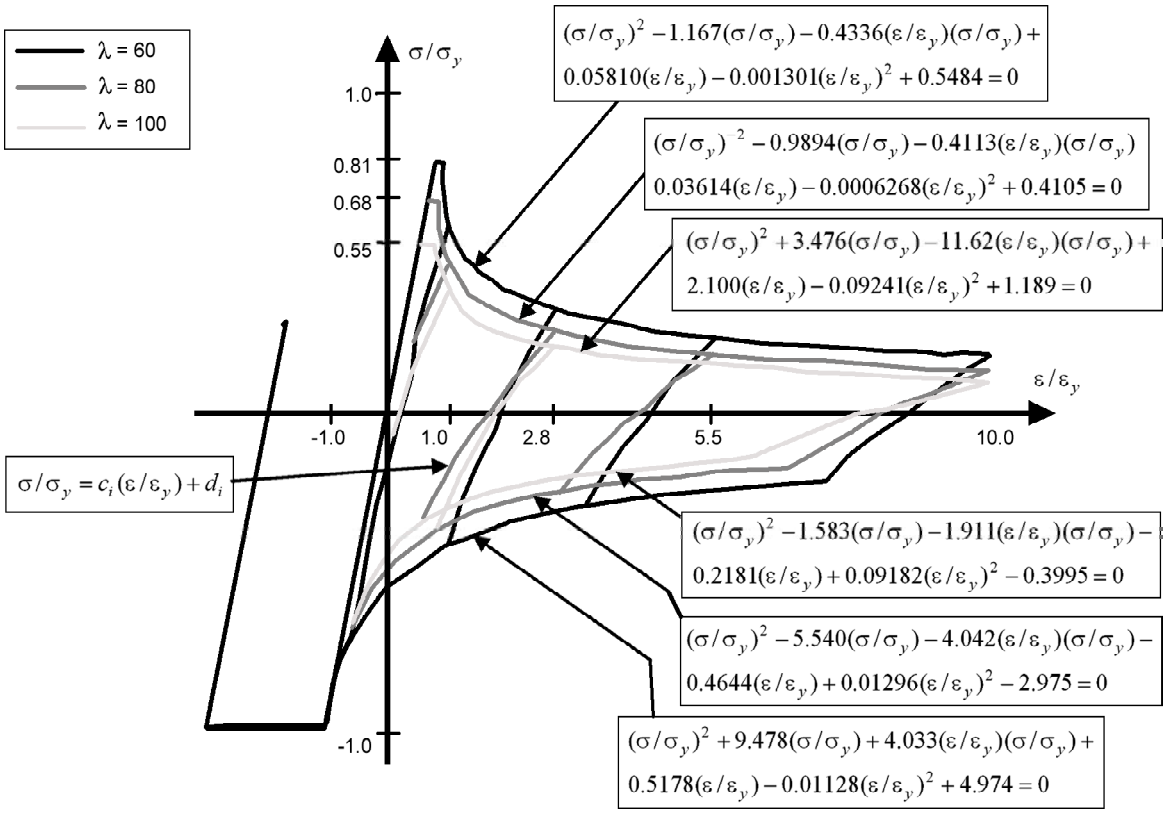


**Figure 9.** Nonlinear post-buckling behavior of bars with slendernesses 60, 80 and 100.

more effective. The reduction in the periods of these structures results in a decrease in responses of the structures, since they generally have low periods and fall in the acceleration constant region of the response spectrum.

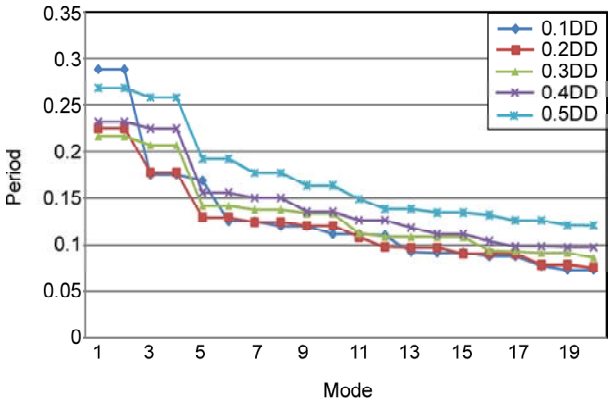


**Figure 10.** Periods of DD models of double layer dome.

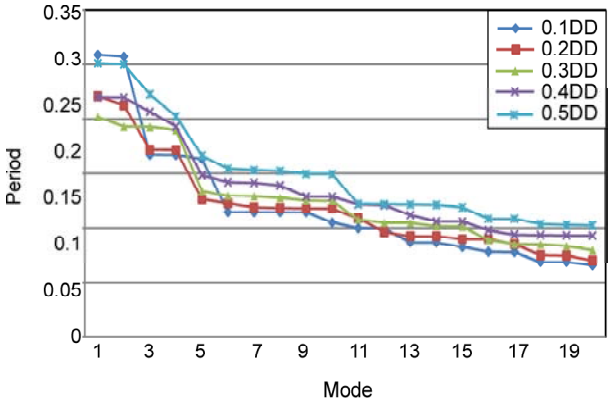


**Figure 11.** Periods of DE models of double layer dome.

### *4.3. Comparison of the Responses of Two Sets of Models*

In the last stage of the research, the dynamic nonlinear responses of two sets of models were compared against the horizontal accelerograms of three earthquakes of El Centro, USA (1943), Kobe, Japan (1995), and Tabas, Iran (1987). The main characteristics of these earthquakes are shown in Table (1). All the accelerograms are scaled to the zone 1 (very high seismic risk region) and soil type 2 of Iranian national code of seismic design of buildings [19].

#### 4.3.1. Domes with Rise to Span Ratio of 0.1

Results of dynamic nonlinear analyses of two DD and DE models with rise to span ratio of 0.1 show that the maximum displacement occurs under the El Centro earthquake for DD model in vertical direction equal to 1.6 cm, Tables (2) and (3). Moreover, Tables (2) and (3) show that there is no sign of buckling in the elements and this implies that these domes, which are shallow domes, are safe enough against horizontal components of earthquakes even without consideration of earthquake loading in their design stage. However, the deflection in the DE model is less than the DD model. This is clearer in horizontal deflection results.

#### 4.3.2. Domes with Rise to Span Ratio of 0.2

Tables (4) and (5) show that the maximum displacement occurs in model DD with rise to span ratio of 0.2 in vertical direction equal to 1.8 cm

**Table 2.** Selected data of responses of DD model with rise to span ratio of 0.1

| (H/S) | ACC | UX (MAX ) | UY (MAX) | UZ (MAX ) | Instance of First Buckling (sec) | No of Buckled Elements | Collapse Time (sec) | Joints IDs | First Buckled Element |
|---|---|---|---|---|---|---|---|---|---|
| 0.1 DD | EL CENTRO | 0.003 | 0.0024 | 0.016 | ******* | ******* | ******* | ux = 168, uy = 174, uz = 73 | ******* |
| | KOBE | 0.00179 | 0.00141 | 0.0098 | ******* | ******* | ******* | ux = 151, uy = 205,uz = 55 | ******* |
| | TABAS | 0.00225 | 0.00147 | 0.012 | ******* | ******* | ******* | 168, 174, 73 | ******* |

**Table 3.** Selected data of responses of DE model with rise to span ratio of 0.1.

| (H/S) | ACC | UX (MAX ) | UY (MAX) | UZ (MAX ) | Instance of First Buckling (sec) | No of Buckled Elements | Collapse Time (sec) | Joints IDs | First Buckled Element |
|---|---|---|---|---|---|---|---|---|---|
| 0.1 DE | EL CENTRO | 0.0016 | 0.00146 | 0.0089 | ******* | ******* | ******* | ux = 184, uy = 192, uz = 65 | ******* |
| | KOBE | 0.00173 | 0.00147 | 0.0096 | ******* | ******* | ******* | 184, 191, 64 | ******* |
| | TABAS | 0.00181 | 0.00149 | 0.0099 | ******* | ******* | ******* | 170, 192, 98 | ******* |

**Table 4.** Selected data of responses of DD model with rise to span ratio of 0.2.

| (H/S) | ACC | UX (MAX ) | UY (MAX) | UZ (MAX ) | Instance of First Buckling (sec) | No of Buckled Elements | Collapse Time (sec) | Joints IDs | First Buckled Element |
|---|---|---|---|---|---|---|---|---|---|
| 0.2 DD | EL CENTRO | 0.00186 | 0.00121 | 0.0048 | ******* | ******* | ******* | 181, 235, 69 | ******* |
| | KOBE | 0.0017 | 0.00119 | 0.0045 | ******* | ******* | ******* | 196, 233, 47 | ******* |
| | TABAS | 0.007 | 0.0051 | 0.018 | t = 3.68 | 19 | ******* | 67, 180, 16 | EL = 121 |

**Table 5.** Selected data of responses of DE model with rise to span ratio of 0.2.

| (H/S) | ACC | UX (MAX ) | UY (MAX) | UZ (MAX ) | Instance of First Buckling (sec) | No of Buckled Elements | Collapse Time (sec) | Joints IDs | First Buckled Element |
|---|---|---|---|---|---|---|---|---|---|
| 0.2 DE | EL CENTRO | 0.00235 | 0.00122 | 0.0062 | ******* | ******* | ******* | 129, 194, 91 | ******* |
| | KOBE | 0.00117 | 0.001175 | 0.0034 | ******* | ******* | ******* | 188, 166, 3 | ******* |
| | TABAS | 0.0064 | 0.0041 | 0.0169 | t = 4.5 | 12 | ******* | 1, 35, 89 | EL = 27 |

under Tabas earthquake. The corresponding displacement for model DE is 1.69 cm. Those tables illustrate that although the buckling in elements does not vanish for model DE, the buckled elements number decrease about 30% in comparison to DD model. Furthermore, the first buckling occurs in later time for model DE. Figure (12) illustrates the post-buckling behavior of the first buckled member for the double layer dome with rise to span ratio of 0.2, which is designed considering earthquake loading.

### 4.3.3. Domes with Rise to Span Ratio of 0.3

According to Tables (6) and (7), the maximum vertical displacement is 1.6 cm in model DD with rise to span ratio of 0.3 and is 1.22 cm in model DE under Tabas earthquake. These tables also show that the number of buckled members for DE model is diminished considerably besides prolonging the buckling time for the first buckled member in DE model. Figures (13) and (14) illustrate the Post-buckling behavior of the first buckled member for models DD and DE, respectively. Comparison of

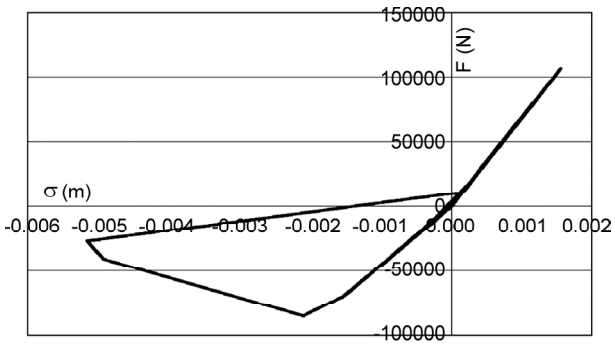


**Figure 12.** Post-buckling behavior of the first buckled element in DE model with rise to span ratio of 0.2 under Tabas earthquake.

**Table 6.** Selected data of responses of DD model with rise to span ratio of 0.3.

| (H/S) | ACC | UX (MAX ) | UY (MAX) | UZ (MAX ) | Instance of First Buckling (sec) | No of Buckled Elements | Collapse Time (sec) | Joints IDs | First Buckled Element |
|---|---|---|---|---|---|---|---|---|---|
| 0.3 DD | EL CENTRO | 0.00035 | 0.00136 | 0.0043 | ******* | ******* | ******* | 105, 217, 151 | ******* |
| | KOBE | 0.0015 | 0.00131 | 0.0024 | ******* | ******* | ******* | 225, 218, 196 | ******* |
| | TABAS | 0.00769 | 0.0123 | 0.0161 | t = 3.94 | 43 | ******* | 29, 61, 61 | EL = 105 |

these two figures implies that the hysteretic energy of DE model is larger than DD model. These results also show that the model designed with consideration of equivalent static earthquake loading act dynamically more dissipating.

### 4.3.4. Domes with Rise to Span Ratio of 0.4

Tables (8) and (9) present the maximum vertical displacements in model DD with rise to span ratio of 0.4 as 2.9 cm under Tabas earthquake. The corresponding figure for DE model is 1.13 cm which is effectively less amount. As the Tables show, the number of buckled elements decreases significantly, but also the first element buckling occurs later for DE model.

Figures (15) and (16) illustrate the post-buckling behavior of the first buckled element for DD and DE models under Tabas earthquake, respectively. Again, DE model show more ability to dissipate the earthquake input energy.

**Table 7.** Selected data of responses of DE model with rise to span ratio of 0.3.

| (H/S) | ACC | UX (MAX ) | UY (MAX) | UZ (MAX ) | Instance of First Buckling (sec) | No of Buckled Elements | Collapse Time (sec) | Joints IDs | First Buckled Element |
|---|---|---|---|---|---|---|---|---|---|
| 0.3 DE | EL CENTRO | 0.0018 | 0.00133 | 0.003 | ******* | ******* | ******* | 46, 157, 45 | ******* |
| | KOBE | 0.00147 | 0.00136 | 0.0024 | ******* | ******* | ******* | 130, 158, 165 | ******* |
| | TABAS | 0.0048 | 0.004 | 0.0122 | t = 7.28 | 18 | ******* | 71, 30, 71 | EL = 30 |

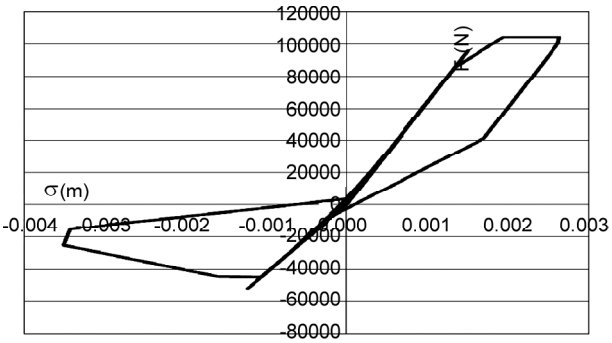


**Figure 13.** Post-buckling behavior of the first buckled element in DD model with rise to span ratio of 0.3 under Tabas earthquake.

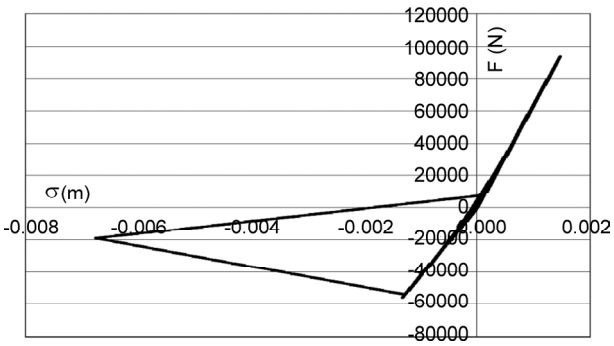


**Figure 14.** Post-buckling behavior of the first buckled element in DE model with rise to span ratio of 0.3 under Tabas earthquake.

**Table 8.** Selected data of responses of DD model with rise to span ratio of 0.4.

| (H/S) | ACC | UX (MAX ) | UY (MAX) | UZ (MAX ) | Instance of First Buckling (sec) | No of Buckled Elements | Collapse Time (sec) | Joints IDs | First Buckled Element |
|---|---|---|---|---|---|---|---|---|---|
| 0.4 DD | EL CENTRO | 0.003 | 0.00098 | 0.0035 | ******* | ******* | ******* | 45, 81, 46 | ******* |
| | KOBE | 0.00149 | 0.00083 | 0.00218 | ******* | ******* | ******* | 31, 54, 31 | ******* |
| | TABAS | 0.027 | 0.0161 | 0.0296 | t = 3.92 | 33 | t = 4.652 | 133, 151, 133 | EL = 16 |

**Table 9.** Selected data of responses of DE model with rise to span ratio of 0.4.

| (H/S) | ACC | UX (MAX ) | UY (MAX) | UZ (MAX ) | Instance of First Buckling (sec) | No of Buckled Elements | Collapse Time (sec) | Joints IDs | First Buckled Element |
|---|---|---|---|---|---|---|---|---|---|
| 0.4 DE | EL CENTRO | 0.0011 | 0.00089 | 0.002 | ******* | ******* | ******* | 46, 53, 46 | ******* |
| | KOBE | 0.00109 | 0.00089 | 0.002 | ******* | ******* | ******* | 60, 53, 31 | ******* |
| | TABAS | 0.00558 | 0.0036 | 0.0113 | t = 4.23 | 11 | ******* | 90, 18, 90 | EL = 16 |

### 4.3.5. Domes with Rise to Span Ratio of 0.5

Considering the Tables (10) and (11), the maximum vertical displacement for DD model with rise to span ratio of 0.5 decreases from 5.8 cm to 2.4 cm for DE model under Tabas earthquake. Besides, these Tables show that not only the number of buckled elements is reduced significantly for the DE models, but the time of first buckling occurrence increases too. Figures (17) and (18) illustrate the post-buckling behavior of the first buckled element

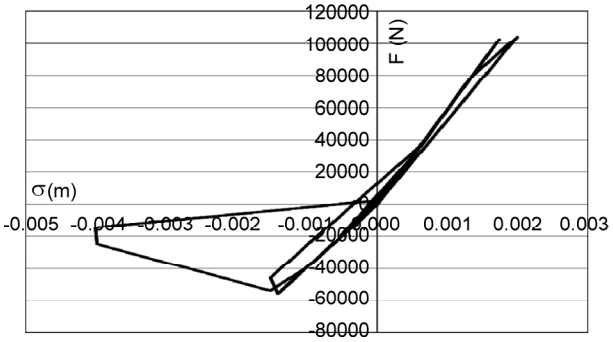


**Figure 15.** Post-buckling behavior of the first buckled element in DD model with rise to span ratio of 0.4 under Tabas earthquake.

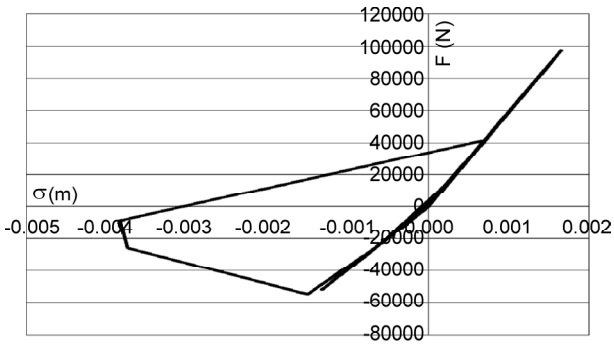


**Figure 16.** Post-buckling behavior of the first buckled element in DE model with rise to span ratio of 0.4 under Tabas earthquake.

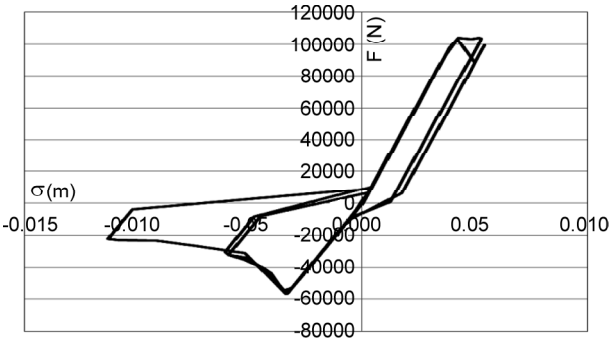


**Figure 17.** Post-buckling behavior of the first buckled element in DD model with rise to span ratio of 0.5 under Tabas earthquake.

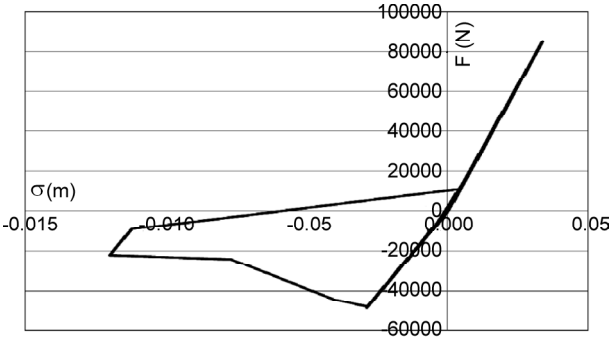


**Figure 18.** Post-buckling behavior of the first buckled element in DE model with rise to span ratio of 0.5 under Tabas earthquake.

**Table 10.** Selected data of responses of DD model with rise to span ratio of 0.5.

| (H/S) | ACC | UX (MAX ) | UY (MAX) | UZ (MAX ) | Instance of First Buckling (sec) | No of Buckled Elements | Collapse Time (sec) | Joints IDs | First Buckled Element |
|---|---|---|---|---|---|---|---|---|---|
| 0.5 DD | EL CENTRO | 0.0021 | 0.001 | 0.0027 | ******* | ******* | ******* | 90,261,90 | ******* |
| | KOBE | 0.0073 | 0.0175 | 0.007 | t = 5.42 | 24 | ******* | 247, 211, 211 | EL = 223 |
| | TABAS | 0.058 | 0.00227 | 0.047 | t = 4.16 | 84 | t = 4.72 | 22, 207, 22 | EL = 256 |

**Table 11.** Selected data of responses of DE model with rise to span ratio of 0.5.

| (H/S) | ACC | UX (MAX ) | UY (MAX) | UZ (MAX ) | Instance of First Buckling (sec) | No of Buckled Elements | Collapse Time (sec) | Joints IDs | First Buckled Element |
|---|---|---|---|---|---|---|---|---|---|
| 0.5 DE | EL CENTRO | 0.00199 | 0.00089 | 0.0028 | ******* | ******* | ******* | 78, 15, 80 | ******* |
| | KOBE | 0.00095 | 0.00088 | 0.0025 | ******* | ******* | ******* | 84, 15, 80 | ******* |
| | TABAS | 0.0167 | 0.011 | 0.024 | t = 3.8 | 37 | ******* | 126, 81, 126 | EL = 71 |

for DD and DE models, respectively. In this case, too, the energy dissipated for DE model is considerably more than DD model.

Therefore, it is shown that consideration of the presented equivalent static earthquake loadings in design of double layer domes improves their safety against earthquake effectively.

## 5. Conclusion

In this research, equivalent static earthquake loading for double layer domes was presented. Then, these equations were applied in the design of some double layer domes and the versatility of these equations is examined through the comparison of the responses of the two sets of domes with and without application of these formulae in their primary design stages. In this regard, the following results are of significance:

- The weight of the domes designed with consideration of presented earthquake loading increases up to 20 percent.
- The displacement of models designed considering equivalent static earthquake loading are less than the other models designed without consideration of these equivalent loads and the difference increases with increase of rise to span ratio of domes.
- The models designed with application of the presented equivalent static earthquake loading buckle later, and the number of buckled elements in these domes is considerably less. In fact, deterministic validation of these equations, like any other equivalent seismic loadings, is impossible. However, since one of the main indices of failure in space structures is due to their bar elements buckling, these equations reduce efficiently this index and make the domes safer against earthquakes.
- With increase in rise to span ratio of double layer domes, the difference of buckled elements in two sets of model increase. Table (12), shows this conclusion in brief.
- The hysteresis loops of the domes responses show that the energy dissipation of domes designed with consideration of equivalent static earthquake action is efficiently larger than the ones designed without consideration of these loads in design stage.
- The equations presented in this paper are only the horizontal action and it seems that complementary formulae should be supplied for vertical action of earthquakes to arise the safety of double layer domes more so that no single element buckles.

## 6. References


1. Saka, T. and Yaniguchi, Y. (1997). Damage to Spatial Structures by the 1995 Hyogoken-Nanbu Earthquake in Japan, *International Journal of Space Structures*, **12**(3-4), 125-133.
2. Kawaguchi, K. (1997). A Report on Large Roof Structures Damaged by the Great Hanshin-Awaji Earthquake, *International Journal of Space Structures*, **12**(3-4), 135-147.
3. Sokol, M. and Sumec, J. (2002). Seismic Response of Large-Span Shell-like Structures, *Fifth International Conference on Space Structures*, Thomas Telford, London, 1037-1042.
4. Malek, S. and Mohyeddin Kermani, A.R. (2002). Three Components Versus Single Component Excitation in the Study of the Seismic behavior of a Triple Layer Grid, *Fifth International Conference on Space Structures*, Thomas Telford, London, 1043-1051.
5. Ishikawa, K. and Kato, S. (1997). Elastic-Plastic Buckling Analysis of Reticular Domes Subjected to Earthquake Motion, *International Journal of Space Structures*, **12**(3-4), 205-216.
6. Lan, T.Y. (2001). Specifications for the Design and Construction of Space Trusses JGJ 7-91, *International Journal of Space Structures*, **16**(3).
7. Sadeghi, A. (2004). Vertical Effects of Earthquakes on the Double Layer Barrel Vaults, *Journal of Space Structures*, **19**(2), 4045-4050.
8. Sadeghi, A. (2004). Horizontal Earthquake Loading and Linear/Nonlinear Seismic Behavior of Double Layer Barrel Vaults, *International Journal of Space Structures*, **19**(1), 21-38.
9. Sadeghi, A. (2010). Effects of Earthquakes on some Families of the Barrel Vaults, LAMBERT Academic Publishing Co., Germany, 443p.

10. Sadeghi, A. and Amani, S. (2012). Investigation of the Benefits of Application of Earthquake Action on the Design of Double Layer Barrel Vaults., *International Journal of Space Structures*, **27**(1), p15.

11. Ma, G. and Yao, Y. (2011). Dynamic Characteristics of a Space Structure Composed of Annular Tensile Cable-Truss Structure and Single Layer Lattice Shell, *Second International Conference on Mechanic Automation and Control Engineering* (MACE).

12. Shen, S., Xing, J., and Fan, F. (2003). Dynamic behavior of Single-Layer Latticed Cylindrical Shells Subjected to Seismic Loading, *Earthquake Engineering and Engineering Vibration*, **2**(2), 269-279.

13. Salajegheh, E. and Mansouri, I. (2010). Seismic Reliability of Double-Layer Grid Space Structures, in Topping, B.H.V., Adam, J.M., Pallarés, F.J., Bru, R., and Romero, M.L.(Editors), *Proceedings of the 10th International Conf. on Computational Structures Technology*, Civil-Comp Press, Stirlingshire, UK.

14. Moghaddam, H.A. (2000). Seismic behaviour of Space Structures, *International Journal of Space Structures*, **15**(2), 119-135.

15. Cai, J.G., Feng, J., Chen, Y., and Huang, L.F. (2008). Study of the Seismic Performance of Space Beam String Structure, *The 14th World Conference on Earthquake Engineering*, Beijing, China.

16. Sadeghi, A. and Sadr-Noormohammadi, A. (2010). Assessing the Equivalent Static Earthquake Loading on the Double Layer Domes, *Proceedings of International Conference on Lightweight Construction & Earthquake*, Kerman, Iran.

17. Ministry of Housing and Urban Development (2006). Iranian National Building Code, Part 6, Minimum Building Loads, Iran, Tehran (In Persian).

18. ANSYS Academic Research, Release 12.0, Help System, ANSYS, Inc.

19. Ministry of Housing and Urban Development (2008). Iranian National Building Code, Part 10, Iranian Code of Practice for Seismic Resistant Design of Buildings Standard No. 2800 3rd Edition, Iran, Tehran (In Persian).

20. CEN, prEN1998-2, EC8-2 (2003). Design Provisions for Earthquake Resistance of Structures, Part 2, Bridges.

22. Chopra, A.K. (2007). Dynamics of Structures, 3rd Edition, Pearson / Prentice Hall Co.